Zeolite favours propionate syntrophic degradation during anaerobic digestion of food waste under low ammonia stress

Laëtitia Cardona, Laurent Mazéas, Olivier Chapleur

1 **Title**

2 Zeolite favours propionate syntrophic degradation during anaerobic digestion of food waste

3 under low ammonia stress

4 **Author names + Affiliations**

5 Laëtitia Cardona[a], Laurent Mazéas [a], Olivier Chapleur [a*]

6 [a]Université Paris-Saclay, INRAE, PROSE,

7 1 rue Pierre-Gilles de Gennes, CS 10030, 92761 Antony Cedex, France

8 laetitia.cardona@inrae.fr

9 laurent.mazeas@inrae.fr

10 olivier.chapleur@inrae.fr

11 ***Corresponding author**

12 **e-mail:** olivier.chapleur@inrae.fr

13 **phone:** +33 1 40 96 65 06

14 **adress :** Université Paris-Saclay, INRAE, PROSE, 1 rue Pierre-Gilles de Gennes, CS 10030,

15 92761 Antony Cedex, France

16 **Declaration of interest: none**

Abstract

Zeolite addition has been widely suggested for its ability to overcome ammonia stress occurring during anaerobic digestion. However little is known regarding the underlying mechanisms of mitigation and especially how zeolite influences the microbial structuration. The aim of this study was to bring new contributions on the effect of zeolite on the microbial community arrangement under a low ammonia stress. Replicated batch experiments were conducted. The microbial population was characterised with 16S sequencing. Methanogenic pathways were identified with methane isotopic fractionation. In presence of ammonia, zeolite mitigated the decrease of biogas production rate. Zeolite induced the development of *Izimaplasmatales* order and preserved *Peptococcaceae* family members, known as propionate degraders. Moreover methane isotopic fractionation showed that hydrogenotrophic methanogenesis was maintained in presence of zeolite under ammonia low stress. Our results put forward the benefit of zeolite to improve the bacteria-archaea syntrophy needed for propionate degradation and methane production under a low ammonia stress.

Keywords

Microbial syntrophy; mineral support; methanogenesis; carbon-isotopic fractionation

1. Introduction

In a context of sustainable energy development, anaerobic digestion (AD) is recognised worldwide as a promising bioenergy technology. It is a multi-steps biodegradation process that has the double advantage to reduce the volume of organic waste and produce at the same time methane-rich biogas, usable in both heat and power generation. However, AD is managed by a complex microbial community that is very sensitive to the modifications of the environmental conditions or the presence of inhibiting molecules. Disruption of the microbial equilibrium inside the anaerobic digesters can have dramatic consequences on their degradation performances.

In particular, ammonia is recognized as one of the inhibitor influencing the most anaerobic digestion process. Ammonia is formed during the degradation of protein-rich substrates such as animal manure, slaughterhouse waste or grass (Mata-Alvarez et al., 2014; Munk et al., 2017). Even if ammonia is an essential nutrient for microbial growth, a concentration beyond 200 mg/L TAN (Total Ammonia Nitrogen) can be harmful for the microorganisms (Chen et al., 2008), and a wide range of ammonia concentrations, from 1.1 to 11.8 gTAN/L or 0.027 to 1.45 gFAN/L (FAN, Free Ammonia Nitrogen), has been reported to half-inhibit methanogenic activity (Capson-Tojo et al., 2020).

To counteract the effect of ammonia on AD performances, different strategies have been studied. Anaerobic co-digestion allows to balance the C/N ratio by mixing at least two substrates, one with a low protein content (Prabhu and Mutnuri, 2016), to reduce the concentration of ammonia formed in the digesters. Stripping allows to capture ammonia in gas bubbles to decrease its concentration in the digesters (Bousek et al., 2016). Bioaugmentation is used to increase the resistance of the microbial community by adding specific cultures (Tian et al., 2019; Yang et al., 2019). Addition of mineral supports such as

natural zeolite has also been proven to mitigate the ammonia inhibition and improve digester performances (Montalvo et al., 2005; Poirier et al., 2017; Tada et al., 2005). However, optimizing these strategies requires a better understanding of the underlying mechanisms of mitigation.

Zeolite presents different properties useful in the mitigation of the inhibition: natural ion-exchange properties, absorptive capacity and could be a support for the biomass (Montalvo et al., 2012). In particular, zeolite naturally contains Na^+, K^+, Ca^{2+} and Mg^{2+} which could stimulate microbial growth or serve as antagonist to NH_4^+ (Chen et al., 2008; Krakat et al., 2017). These ion-exchange and absorptive capacities could be improved by modifying physically or chemically the zeolite (Ates and Hardacre, 2012; Zhang et al., 2019). For example, Zhang et al (2019) used lignite-modified zeolite that adsorbed ammonium and improved by 7 times the methane production in digesters inhibited by ammonia. They also demonstrated a higher biomass immobilisation using the modified zeolite, but provided no further information regarding the identity of these microbes. In general, the role of zeolite in the immobilisation of the biomass has been mainly evidenced using electronic microscopy (Fernández et al., 2007). Weiß et al showed that hydrolytic microorganisms such as *Ruminofilibacter xylanolyticum* and methanogenic archaea could grow on zeolite under non inhibiting conditions (Weiß et al., 2013, 2011).

However, only a few studies investigated the consequences of natural zeolite addition on microbial structuration during ammonia inhibition and related it to the performances of the digester. In digesters inhibited by 19 g-TAN/L, Poirier et al. observed that methane production could be increased by 39% and lag phase reduced by 50% when zeolite was added. This mitigation was associated to the preservation of archaea *Methanosarcina* and development of *Methanobacterium* (Poirier et al., 2017). However, clear role of the zeolite was not understood. For this reason, in the present work we focused on the identification of

the microbes influenced by the presence of natural zeolite under ammonia inhibition and on the role of the zeolite on specific microbial degradation pathways.

Microbial community structure was evaluated with 16S metabarcoding and linked to the digester performances. Two series of lab digesters were set up: a control series without ammonia and a stressed series with ammonia. In the stressed series, 4 g-TAN/L were added in order to induce a low stress and simulate a bioprocess at an early stage of ammonia accumulation. If multiple studies have been carried out in order to determine the mitigation effect of the zeolite under medium to high ammonia inhibition (Poirier et al., 2017; Wang et al., 2011), a few studies also demonstrated that zeolite improves the methane production under low ammonia inhibition (Milán et al., 2001; Wijesinghe et al., 2019), but did not collect information regarding the microbial communities.

Different pre-treatments were applied to the zeolite to test different hypotheses on its role on the microbial community structuration. The influence of fine particles release was tested (Abadzic and Ryan, 2001). For that purpose the zeolite was boiled to release directly soluble particles into water. Effects of both the modified zeolite and the obtained solution were tested. The effect of an increase of the surface available was also evaluated by pre-treating thermically the zeolite to remove water and free sites. By removing the adsorbed water, the adsorptive capacity of the zeolite could be improve (Kesraoui-Ouki et al., 1994) as well as microbial growth by increasing the surface. In total, for each series, 5 zeolite conditions were tested.

2. Material and Methods

2.1. Feedstock preparation

The inoculum used in the experiment came from a mesophilic lab-scale anaerobic digester (60L) treating biowaste. In order to degrade the residual organic matter in excess it

was stored at 35°C during two weeks in anaerobic condition without feeding before being used. The inoculum was centrifuged at 10,000g during 10 minutes before use.

The substrate used to feed the digesters came from an industrial food waste collector (Valdis Energie, Issé). The food waste came from different origin such as schools, markets and expired products. The food waste was crushed before use.

The physico-chemical characteristics of the inoculum and biowaste are presented in the supplementary material.

2.2. Preparation of zeolite

Zeolite was obtained from Somez society (France). The zeolite was sieved to obtain a homogeneous size between 0.48-0.50 mm. To release easily soluble ions a part of the zeolite was boiled at 100°C in water during 20 minutes. The liquid residue, containing the easily soluble ions, was filtered at 0.22 µm before use and residual solid part was dried before use. To increase the surface availability for microbial colonisation and modify the ion-exchange capacity another part of the zeolite was heated in the oven at 400°C during 4 hours.

2.3. Experimental set-up

Table 1 summarises the composition of the different digesters. In total 30 anaerobic batch bioreactors were set-up in 1 L glass bottles (700mL working volume). Each digester was inoculated with methanogenic sludge and fed with biowaste to reach a substrate/inoculum ratio of 12 g COD/1,2 g COD. Zeolites previously prepared were added at a concentration of 15g/L measured before pre-treatment. In parallel a control without zeolite was set-up. In total 5 conditions were tested in triplicate. Ammonium carbonate (Alfa Aesar) was added to reach a concentration of 4 g/L of TAN. In parallel to the series with ammonia (N series) a control series without addition of ammonium carbonate (C series) was set-up. All the digesters were complemented with a biochemical potential buffer (International Standard ISO 11734 (1995))

131 to reach a final working volume of 700 mL. To obtain an equal quantity of carbonate in the
132 different digesters, sodium carbonate was added into the BMP for the control C series. The
133 bioreactors were then sealed with a screw cap and a rubber septum. The headspaces were
134 flushed with N_2 (purity >99.99%, Linde gas SA) and the bottles were incubated at 35°C in the
135 dark and without agitation.

136 Weekly, 6mL of liquid phase were sampled through the septum using a syringe and
137 centrifuged at 10,000 g for 10 minutes. Supernatant and pellet were snap frozen using liquid
138 nitrogen and kept at -20°C and -80°C respectively.

139
140

141 *2.4. Gas production and chemical analyses*

142 The different parameters such as biogas composition, NH_4^+/NH_3, volatile fatty acids
143 were measured as described in (Cardona et al., 2019; Chapleur et al., 2014).

144 Production parameters were calculated using R CRAN software and the Gompertz
145 equation with R Grofit package.

146 $$y(t) = A.\exp[-\exp\left(\frac{\mu.e}{A}(\lambda - t) + 1\right)]$$

147 Where y(t) is the cumulative CH_4 production (mgC) at date t, A is the ultimate CH_4
148 production (mgC), μ is the maximum CH_4 production rate (mgC/day), and λ is the lag phase
149 (days).

150 The link between Free Ammonia Nitrogen (FAN), Total Ammonia Nitrogen (TAN), pH
151 and temperature can be summarized with the following equation (Anthonisen et al., 1976):

152 $$FAN = \frac{10^{pH}}{(\exp\left(\frac{6344}{T}\right) + 10^{pH})} x\ TAN$$

153 Where T is the temperature in Kelvin.

2.5. *Isotopic fractionation*

As indicator of the methanogenic pathway the isotopic fractionation of the CH_4 ($\delta^{13}C$-CH_4) was measured using a Trace Gas Chromatograph Ultra (Thermo Scientific) attached to a Delta V Plus isotope ratio mass spectrometer via a GC combustion III (Thermo Scientific). Periodically gas was sampled into 7-mL vacuumed serum tubes for the analysis. It is assumed that a value of $\delta^{13}C$-CH_4 inferior to -60‰ indicates a CH_4 production through the hydrogenotrophic pathway and a value of $\delta^{13}C$-CH_4 superior to -60‰ indicates a CH_4 production through the acetoclastic pathway (Whiticar et al., 1986).

2.6. *Analysis of the microbial community*

Total DNA was extracted from sample's pellet using DNeasy PowerSoil kit (QIAGEN) following the manufacturer instructions. The DNA quantity was measured by Qubit (dsDNA HS assay kit, Invitrogen).

Archaeal and bacterial hyper variable region V4-V5 of the 16S rRNA gene was amplified by PCR with fusion primers 515F (5′- Ion A adapter–Barcode–GTGYCAGCMGCCGCGGTA-3′) and 928R (5′-Ion trP1 adapter–CCCCGYCAATTCMTTTRAGT-3′), which include a barcode and sequencing adapters, and then sequenced according to the protocol described by Madigou et al. (2019).

2.7. *Data analyses*

2.7.1. Gas production

The variance between the biogas productions observed under the different conditions was estimated by comparing the 3 Gompertz parameters calculated for both CH_4 and CO_2 with analysis of variance (ANOVA). The function *granova.1w* from the R package *granova* (version 2.1) was used to compute the ANOVA. This package provides a graphical

177 representation of the ANOVA results. For each parameter tested (6 in our case), one graphic
178 represents on the y-axis the individual and mean value of the parameter for each condition
179 (C0, C1, C2, C3, C4, N0, N1, N2, N3, and N4), classified on the x-axis according to the
180 estimated contrast coefficient for each condition. The contrast coefficient is calculated as the
181 difference between the group mean (mean of all the digesters of the condition) and the grand
182 mean (mean of all the digesters). This representation enables to visualise at the same time the
183 variation within and between the groups. In addition the graphic represents the mean square
184 error between the conditions (MS-between) and the mean square error within the conditions
185 (MS-within) in the form of squares. The comparison between the area of the MS-between and
186 the area of the MS-within indicates if some conditions are significantly different form the
187 others. The F-statistic value is also indicated on the graph. This value is calculated as the ratio
188 of the area of the MS-between and the area of the MS-within. Combined to the p-value, the F-
189 statistic value (F>1) allows to determine if there is a significant difference in the mean
190 between the conditions for the different Gompertz parameters. Finally the residuals, portions
191 of the variability unexplained by the ANOVA, are also represented. The repartition of the
192 residuals indicates if the residuals are independent or not and confirm if the dataset meets the
193 assumptions of the ANOVA (independence, normality, homogeneity).

194 2.7.2. Microbial dynamics

195 An OTU count matrix was designed using FROGS (Find Rapidly OTU with Galaxy
196 Solution), a galaxy/CLI workflow (Escudié et al., 2018). The OTUs abundances were
197 examined through statistical analyses using R CRAN software (version 3.5.1). Low abundant
198 OTUs were filtered: OTUs present above 1% in at least one sample were kept. OTUs
199 abundances in the samples were finally transformed with centered log ratio (CLR) (Lê Cao et
200 al., 2016).

201 Multivariate analyses were computed using mixOmics R package (version 6.6.1)
202 (Rohart et al., 2017). Firstly, Principal Component Analysis (PCA) was performed to
203 highlight the relationship between samples from the different conditions (ammonia/zeolite).
204 Secondly, sparse Partial Least Square Discriminant Analysis was carried out to compare the
205 different conditions and evidence the microorganisms influenced by the presence of ammonia
206 and/or zeolite. More precisely, three pairwise sPLS-DA were carried out respectively between
207 the control C series and N series without zeolite (N0-N1); between N series without and with
208 solid zeolite (N1-N3-N4) and between C series and N series with solid zeolite. The
209 abundances of the most discriminant microorganisms selected by the three sPLS-DAs were
210 summarised in a heatmap using Euclidean distance and ward clustering method.

211 **3. Results and discussion**

212 *3.1. Modification of the performances of anaerobic digestion*

213 Differences in CH_4 and CO_2 productions could be observed between the digesters from
214 N and C series (supplementary material). To compare them accurately between the different
215 experimental conditions, each gas production curve was modelled with the Gompertz
216 equation (the estimated Gompertz parameters are summarised in the supplementary material).
217 The variance of the estimated Gompertz parameters between each condition was evaluated
218 using ANOVA. Results are summarized in Figure 1. We first observed that, for all the
219 parameters, calculated residuals were randomly distributed. It showed that the assumptions of
220 ANOVA were met and that ANOVA results could be trusted. For all the parameters the p-
221 value and F-statistic values were significant ($p\text{-value}<0.05$ and $F>1$) which meant that at least
222 one of the conditions was significantly different from the others. The different conditions
223 were then compared by groups to evidence the effect of ammonia and zeolite on the
224 production of biogas.

225

226 3.1.1. Effect of a low concentration of ammonia on biogas production

227 Regarding CO_2 production (figure 1-A-B-C), the presence of ammonia, independently
228 of zeolite addition (N series), resulted in a decrease of the maximal production (from 499 to
229 270 mgC for the extreme values) and of the production rate (from 19.8 to 9.6 mgC/day for the
230 extreme values) compared to C series. In addition the lag phase increased from 0 to 5.8 days
231 between the digesters from the C and N series.

232 Regarding the CH_4 production (figure 1-D-E-F), the presence of ammonia resulted in an
233 increase of the maximal production (from 895 to 1005 mgC for the extreme values). However
234 the lag phase increased from 5.8 to 9 days for respectively the C series and the conditions N0
235 and N2 (without zeolite). No general trend was observed for CH_4 production rate.

236 The comparison of the CH_4 and CO_2 production values indicated that the presence of a
237 low concentration of ammonia slowed down the process, even if no strong inhibition was
238 observed. This was expected as the objective of the study was to investigate the effect of the
239 zeolite during the early stage of ammonia accumulation. The operational performances were
240 even improved as production of CH_4 increased in presence of ammonia. One hypothesis is
241 that ammonia stressed the acetoclastic archaea in favour of the hydrogenotrophic ones,
242 leading to an enrichment of the biogas into methane. This hypothesis is supported by different
243 authors (Lv et al., 2018; Ruiz-Sánchez et al., 2019; Westerholm et al., 2011).

244 3.1.2. Effect of zeolite in presence of ammonia (N series)

245 Based on the lag phase and production rate of the CH_4 and CO_2 production, the
246 digesters of N series could be separated in two groups. A first group was composed of N0 (no
247 zeolite) and N2 (liquid residue). A second group was composed of the digesters with solid
248 zeolite, no matter the treatment (N1-N3-N4).

249 The presence of solid zeolite (N1-N3-N4) allowed to decrease the lag phase by 2 days
250 for both CO_2 and CH_4 and to increase the production rate by 1.2 times compared to N0-N2.
251 Similarly, Poirier et al (2017) used a similar natural zeolite and observed a reduction of the
252 lag phase by 20 days for CH_4 production and 39% improvement of the maximal production in
253 digester inhibited with 19g/L of TAN. In that case effect of zeolite was greater, probably
254 because the level of stress imposed was also greater.
255 Boiling the zeolite was done in order to release fine particles from the zeolite. The
256 removed particles do not seem to be the mechanism behind the inhibition mitigation in the
257 conditions of our experiment. Heating the zeolite was done in order to remove water and
258 organic residues and release free sites to improve molecules adsorption or microbial
259 colonisation. Increasing the surface on the zeolite did not improve the performances. This
260 could be due to a limited growth of microorganisms in the duration of the experiment which
261 did not saturate the surface of the zeolite in N1 and did not benefit from the increased surface
262 in N4. In order to evidence the microbial colonisation of the zeolite, electronic microscopy
263 could be applied as described in several studies (Fernández et al., 2007; Zhang et al., 2019).
264 In all cases solid zeolite mitigated ammonia stress. It may have acted as a support for
265 the microbial growth and/or improved the microbial interaction by decreasing the spatial
266 distance between microorganisms engaged for example in a syntrophy.

267 3.1.3. Effect of zeolite without ammonia (C series)

268 Regarding the digesters without ammonia addition (C series) biogas performances were
269 not significantly different between the conditions. Indeed the CH_4 and CO_2 maximal
270 production were respectively close to 925 ±27.8 and 487 ±8.9 mgC for all the digesters.
271 Compared to the control (C0), the CH_4 production rate was slightly reduced in presence of
272 solid zeolite (C1-C3-C4) and liquid residue (C2), from 47 mgC/day for the control to 42-46
273 mgC/day for solid zeolite and 38 mgC/day for liquid residue. However the lag phase was not

modified between the reactors. This result is in accordance with previous study showing that the presence of the zeolite in absence of ammonia had little influence on the digesters performances (Poirier et al., 2017).

3.2. Effect of zeolite treatments on different chemical parameters

The Figure 2 summarises the evolution of the acetate, propionate and butyrate concentrations, pH, Free Ammonia Nitrogen (FAN) and Total Ammonia Nitrogen (TAN) concentration for the different conditions.

3.2.1. Ammonia evolution

In the digesters of the C series, the ammonia concentration remained under 200 mg-TAN/L (10 mg-NH_3/L). In the digesters of N series, the TAN concentration remained stable around 4000 mg/L all along the experiment. The concentration of ammonia did not decrease across the experiment in presence of zeolite. This confirmed that the adsorption of ammonia by the zeolite remained limited in our experiment.

The free ammonia nitrogen (FAN) concentration rapidly stabilised at 300 mg-NH_3/L in the digesters of the N series even if it was higher than 1000 mg-NH_3/L at the beginning of the experiment. This decrease was due to a drop of pH, consequence of the VFAs accumulation observed for all the digesters. It is usually assumed that the FAN is the most toxic form of ammonia for the methanogens community. Several studies reported an inhibitory threshold between 50 to 1400 mg-NH_3/L (Astals et al., 2018; Rajagopal et al., 2013). In our case, the first days at a high concentration of FAN was probably the most stressful for the microorganisms. This can explain the delay observed in the biogas production in presence of ammonia. However, after a few days, decrease of pH resulted in the expected low ammonia stress in the digesters of N series.

3.2.2. Volatile fatty acids evolution

All the digesters in absence of ammonia (C series) presented the same VFA evolution. The maximum accumulation was around 750 mgC/L, 350 mgC/L and 300 mgC/L for respectively acetate, propionate and butyrate. No effect of zeolite was observed in that case.

Under low ammonia stress, the VFA accumulations confirmed the grouping of the different conditions from the N series observed with the gas production (N0-N2 and N1-N3-N4).

In presence of ammonia and without solid zeolite (N0-N2) higher acetate (1050 mgC/L) coupled to lower propionate (200 mgC/L) and butyrate (150 mgC/L) accumulations than in digesters from C series was observed. The acetate can be degraded by acetoclastic archaea or bacteria in syntrophy with hydrogenotrophic archaea. The increase of the acetate accumulation observed in these digesters could be due to the stress of the acetoclastic archaea by the ammonia, as observed in previous studies (Wang et al., 2015). On the other hand, both propionate and butyrate require syntrophy for their degradation (Müller et al., 2010). Their lower accumulation in presence of ammonia suggested that syntrophic archaea were not inhibited. This is contradictory with several studies that evidenced that ammonia could inhibit the syntrophic propionate degrading bacteria (SPOB) and methanogens leading to an accumulation of propionate (Calli et al., 2005; Zhang et al., 2018). However in our study the stress was lower than in the cited studies (4 gTAN/L versus 7 gTAN/L in Zhang et al 2018) which could explain the difference in the propionate and butyrate degradation. The complete propionate degradation was achieved at day 40 such as in the C series. Consequently, as suggested by the biogas composition and the accumulation of acetate, we hypothesized that the acetoclastic methanogens were delayed in favour of the hydrogenotrophic methanogens in N0-N2. This succession of events may have favoured the syntrophic degradation of the butyrate and propionate in presence of ammonia.

In presence of ammonia and with solid zeolite (N1-N3-N4) the pattern of evolution of the butyrate was similar to the one of N0-N2, while acetate and propionate evolutions were similar to the one in C series, except that the propionate was fully consumed earlier. It can be hypothesized that the zeolite limited the perturbation of the acetoclastic archaea by NH_3. The preservation of the activity of the acetoclastic methanogens allowed to consume the acetate faster than in presence of ammonia. The high activity of the acetoclastic archaea may have limited the growth of the hydrogenotrophic archaea resulting in higher accumulation of propionate than in N0-N2. However, butyrate did not accumulate. We hypothesized that a competition for the syntrophy with the hydrogenotrophic archaea was won by the butyrate degraders, explaining this low accumulation. It would be in accordance with thermodynamic observation that the Gibbs free energy needed for the propionate degradation is higher than the one for the butyrate degradation, and makes it harder to degrade (Wu et al., 2016). However, due to the presence of the zeolite, the propionate degradation occurred faster than in absence of zeolite (N0-N2). This means that the presence of zeolite played a significant role on the propionate degraders activity and the syntrophic interactions needed for the VFAs degradation.

3.3. Effect of the ammonia and zeolite on the methanogenic pathways

The methanogenic pathways for the different conditions were evaluated by measuring isotopic fractionation of the CH_4 ($\delta^{13}C$-CH_4) (Figure 3). In absence of ammonia (C series) in all the experiments the $\delta^{13}C$-CH_4 increased from -55 ‰ to -35 ‰ during the degradation of acetate (day 0 to day 30). This progressive increase indicates that the acetate degradation was mainly due to acetoclastic archaea. During propionate degradation the value decreased to -55 ‰ and stabilised at this level until the end of the experiment (day 30 to day 100). It confirmed that propionate degradation implied hydrogenotrophic archaea. The CH_4 produced by their activity led to the dilution of CH_4 produced by acetoclastic archaea.

In presence of ammonia (N series) with or without zeolite the $\delta^{13}C\text{-}CH_4$ was lower at the beginning of the degradation than for the C series. The $\delta^{13}C\text{-}CH_4$ increased from -70 ‰ to -45 ‰ and -35 ‰ respectively for the digesters N1-N3-N4 (with zeolite) and N0-N2 (without solid zeolite) during acetate degradation. This indicates that, at the beginning of the experiment, the acetoclastic pathway was minored in favour of the hydrogenotrophic pathway. This result is in line with the lower CO_2 production observed, as CO_2 was used by the hydrogenotrophic archaea for CH_4 production. After 15 days two types of patterns were observed, grouping the digesters N0-N2 on one side and N1-N3-N4 on the other side, as observed with the previous chemical data.

In absence of zeolite when ammonia was present (N0-N2) the $\delta^{13}C\text{-}CH_4$ reached the same value than the control without ammonia (-35 ‰) at day 33. The propionate degradation then led to the decrease of the $\delta^{13}C\text{-}CH_4$ until -50 ‰. In contrast with the stability in the isotopic composition observed for C series once all the propionate degradation was achieved, a further decrease in the isotopic composition for the N0-N2 digesters was observed until -60 ‰. This result suggests that a mix of both methanogenic pathways seemed to occur under ammonia inhibition without zeolite. This result is in line with a previous study from Ruiz-Sanchez et al (2018). The authors observed a mix of the methanogenic pathways at an ammonia level of 1.9 g-TAN/L (Ruiz-Sánchez et al., 2018).

In presence of zeolite and ammonia (N1-N3-N4) the $\delta^{13}C\text{-}CH_4$ increased until -35 ‰ at day 25. The propionate degradation led to a rapid decrease of the $\delta^{13}C\text{-}CH_4$ to -60 ‰. The value continued to decrease to reach a final value of -65 ‰. The lower increase of the $\delta^{13}C\text{-}CH_4$ compared to the digesters without zeolite N0-N2 indicates that a more important part of the CH_4 was produced by the hydrogenotrophic pathway even if acetoclastic archaea were active.

These results indicate that the acetoclastic archaea were sensitive to the presence of ammonia even at the low concentration used in our experiment. Acetoclastic archaea are usually considered as the most sensitive methanogens to ammonia (Yenigün and Demirel, 2013) and a switch from acetoclastic to hydrogenotrophic methanogenesis is typically observed when ammonia exceeds a threshold of 0.14-0.28 gNH_3/L (3.0-3.3 gNH_4^+-N/L) (Westerholm et al., 2016). In addition ammonia can induce the production of CH_4 through the Syntrophic Acetate Oxidation (SAO) (Schnurer and Nordberg, 2008). Acetoclastic archaea were able to partly overcome this stress when NH_3 concentration decreased due to the VFAs accumulation. However, the presence of zeolite in the digesters enabled an important activity of the hydrogenotrophic archaea leading to a fast degradation of the VFAs and an enrichment of CH_4 in the biogas.

3.4. Identification of the key phylotypes of the different conditions

The microbial community was analysed with 16S RNA metabarcoding for each digester at one time point (day 22) corresponding to the peak of CH_4 production in all the digesters (supplementary material).

Microorganisms specifically influenced by the presence of ammonia and/or zeolite were characterised using sPLS-DA. This method allows the classification of the samples into groups and allows the identification of the key microorganisms discriminating these groups. To evidence respectively microbes discriminant of digesters inhibited by ammonia and not inhibited, of digester containing zeolite or not in presence of ammonia, of digesters without ammonia and digesters with ammonia but containing zeolite, three pairwise sPLS-DA were carried out between the following groups: A (samples from the C series), B (samples from N0-N2 conditions) and C (samples from N1-N3-N4 conditions). The samples could be

398 classified into the different groups with a mean error rate inferior to 4%. Abundances of the
399 key microorganisms characteristic of the different groups and selected through the different
400 sPLS-DA are summarised in a heatmap (Figure 4). The corresponding taxonomic affiliation is
401 reported in the supplementary Table A.3. The microorganisms could be grouped in 5 clusters
402 according to the presence of the zeolite and ammonia.

403
404

405 3.4.1. Microorganisms inhibited by the presence of ammonia

406 The cluster 1 grouped together the microorganisms abundant in the group A (without
407 ammonia) and less abundant in presence of ammonia no matter the presence of zeolite. Seven
408 OTUs belonging to the families *Lachnospiraceae*, *Rikenellaceae, Bacillaceae, Clostridiaceae*
409 and to the order *Bacteroidales* (GZKB124) were identified. *Lachnospiraceae* family is
410 recognised as cellulolytic degrader and is known to produce large amounts of acetate and CO_2
411 (Florentino et al., 2019). *Rikenellaceae* family is known to use lactate fermentation where
412 acetate and propionate are the end-products (Yi et al., 2014). *Clostridiaceae* and
413 *Bacteroidales* are usually reported to be the main phyla in the anaerobic digesters and are
414 known to be cellulolytic microbes (Hassa et al., 2018). In presence of ammonia,
415 microorganisms of cluster 1 were probably replaced by microorganisms with similar
416 functions.

417 3.4.2. Microorganisms preserved under ammonia low stress by the presence of zeolite

418 The cluster 2 grouped the microorganisms present in group A, inhibited by the
419 ammonia (group B) but preserved thanks to the presence of zeolite (group C). Nine OTUs
420 were found and belong to the families *Peptococcaceae, Spirochaetaceae, Lachnospiraceae,*
421 *Cloacimonadaceae, Izimaplasmatales* order and the *Methanoculleus* genus.

Cloacimonadaceae are known to be acetogens (Lee et al., 2018). Members of the family *Peptococcaceae* are syntrophic obligate propionate oxidizers (Ziganshin et al., 2011). The presence at day 22 of this microorganism in group A and C was in accordance with the degradation pattern of the propionate. Indeed in digesters without ammonia and with ammonia and zeolite (group A and C) the propionate degradation occurred earlier than in digesters with ammonia and no zeolite (group B). OTU from genus *Treponema* (*Spirochaetaceae* family) was identified. Some members of this genus are known to degrade cellulose and some others to be homoacetogens and reduce H_2 and CO_2 into acetate (Lee et al., 2013). Finally *Izimaplasmatales* from the *Tenericutes* phylum was described recently by Skennerton et al (Skennerton et al., 2016). It was identified from methane seep sediment samples. The members of *Izimaplasmatales* order are able to ferment anaerobically simple sugars. To the best of our knowledge this study is the first one reporting the presence of *Izimaplasmatales* order in anaerobic digesters. Further analyses should be done to fully understand its role in anaerobic digesters.

3.4.3. Microorganisms whose development results from the presence of ammonia

The cluster 3 grouped the microorganisms which were absent in the group A but abundant in the groups B and C, meaning that their development was favoured by the presence of ammonia, independently of the presence of zeolite. The microorganisms from this cluster, represented by 9 OTUs, belonged to the same families than the one identified in the previously described clusters *Lachnospiraceae*, *Peptococcaceae*, *Clostridiaceae, Izimaplasmatales* and also to *Syntrophomonadaceae*. *Syntrophomonadaceae* family degrades long chain fatty acids into acetate and glycerol (Sousa et al., 2009) but members of the *Syntrophomonas* genus, identified in this system, are butyrate degraders (Narihiro et al., 2016; Zou et al., 2003). The development of this *Syntrophomonas* could explain the faster butyrate degradation observed in the groups with ammonia no matter the presence of zeolite (groups B

447 and C). Moreover, *Syntrophomonas* was already shown to be resistant to the increase of
448 ammonia in CSTR experiment (Bonk et al., 2018). In general, we hypothesized that
449 microorganisms of cluster 3 had similar metabolisms than microorganisms of cluster 1.
450 Switch from one cluster to the other could derive from the presence of ammonia. It could
451 explain the relative similarity of the VFA patterns observed in the reactors no matter the
452 condition.

453 3.4.4. Microorganisms slightly inhibited by the presence of ammonia

454 The cluster 4 grouped the microorganisms more abundant in group A than in groups B
455 and C. Seven OTUs were identified in this cluster and belonged to the families
456 *Dysgonomonadaceae, Synergistaceae* and *Syntrophomonadaceae. Dysgonomonadaceae*
457 family is composed by three genera, *Fermentimonas*, *Petrimonas* and *Proteiniphilum*, which
458 have fermentative activities and produce acetate (Hahnke et al., 2016). *Synergistaceae* family
459 is composed of amino acid degraders (Rivière et al., 2009). All the *Syntrophomonadaceae*
460 present in this cluster belonged to the genus *Syntrophomonas*. Members of this genus seemed
461 to be differently influenced by the presence of ammonia as in cluster 3 another OTU of this
462 genus was favoured by the presence of ammonia. This result is supported by a previous study
463 where a reorganisation within the *Syntrophomonas* population was observed due to the
464 presence of ammonia (Poirier et al., 2020).

465 3.4.5. Microorganisms whose development is enhanced by the presence of ammonia

466 The cluster 5 grouped microorganisms more abundant in groups C and B than in group
467 A. Their relative abundance was increased by the presence of ammonia. Mostly archaea were
468 identified in this cluster, with three bacteria. Identified archaea belonged to the genera
469 *Methanoculleus, Methanobacterium* and *Methanosarcina.* If these genera seemed to be
470 present in the different conditions, the OTUs *Methanobacterium_41, Methanoculleus_2* and
471 *Methanosarcina_1* were specifically favoured by the presence of ammonia. These 3 archaea

472 are known to be resistant to the presence of ammonia (Jarrell et al., 1987; Poirier et al., 2016;
473 Tian et al., 2019). *Methanoculleus* and Methanobacterium are hydrogenotrophic archaea
474 while *Methanosarcina* is a versatile archaea able to use both acetoclastic and
475 hydrogenotrophic pathways. Unfortunately, no additional information at the species level was
476 available from the sequencing results. The modification of archaea species, specifically for
477 *Methanosarcina*, was already observed when ammonia concentration was increased (Poirier
478 et al., 2016). Bacteria belonged to *Marinilabiliaceae* and *Paludibacteraceae* families and to
479 the order *Clostridiales*. Members of *Paludibacteraceae* family use various sugars to produce
480 acetate and propionate as major end-products (Ueki et al., 2006).

481 *3.5. Biological pathway reconstruction*

482 To evidence the effect of zeolite addition in presence of a low concentration of
483 ammonia we summarized the characteristics of AD in the different situations observed (no
484 ammonia, ammonia with solid zeolite, ammonia without solid zeolite). The figure 5 represents
485 for each situation the patterns of VFA degradation and methane production evidenced from
486 the performances analyses, as well as the microbes that could be responsible of these patterns.

487
488

489 In control conditions without ammonia and no matter the zeolite treatments (C series)
490 different VFAs producers were identified such as *Lachnospiraceae*, *Cloacimonadales*,
491 *Rikenellaceae or Spirochaetaceae*. The degradation of the VFA, especially propionate and
492 butyrate, was mainly due to respectively the families *Peptococcaceae* and
493 *Syntrophomonadaceae*. The biogas was composed of 66% of CH_4 and 34% of CO_2. The main
494 pathway for the CH_4 production was the acetoclastic one. It was confirmed by the isotopic
495 fractionation and the patterns of VFAs degradation.

In presence of ammonia and without zeolite (N0-N2) the VFA production was mainly due to *Paludibacteraceae* and *Lachnospiraceae.* The genus *Syntrophomonas*, responsible of the butyrate degradation, was observed indicating its ability to develop in presence of ammonia. The main pathway for methanogenesis before day 15 was the hydrogenotrophic one as the acetoclastic archaea were stressed by the presence of NH_3 (1000 mg-NH_3/L). After day 15, the NH_3 concentration decreased, the acetoclastic archaea overcame the stress and the CH_4 was produced through both hydrogenotrophic and acetoclastic pathways. The relative abundance of specific OTUs of *Methanosarcina*, *Methanoculleus* and *Methanobacterium*, was enhanced by the presence of ammonia. The presence of the bacteria *Marinilabiliaceae* was observed but no specific role could be attributed to this organism in our system.

In presence of ammonia and with zeolite (N1-N3-N4) the VFA production could mainly be attributed to the families *Spirochaetes* and *Cloacimonadaceae.* The hydrogenotrophic pathway seemed to be preserved more importantly than in absence of zeolite. The preservation of the hydrogenotrophic archaea led to a faster degradation of the VFAs in syntrophy with bacteria, such as *Peptococcaceae* and *Syntrophomonas*, respectively propionate and butyrate degraders. The same genera of archaea than the one observed in presence of ammonia only, *Methanosarcina*, *Methanoculleus* and *Methanobacterium,* were also observed in presence of ammonia only. *Izimaplasmatales,* identified only in presence of zeolite could play a role in the performance modification; however we could not put forward any hypothesis on its role due to the lack of knowledge on this microorganism. The development of the family *Marinilabiliaceae* was maintained in presence of zeolite.

In our study the presence of ammonia, even at a low concentration, led to an important dynamics of obligate syntrophic bacteria and hydrogenotrophic archaea. Zeolite could act as a support for the microbial growth which improved the proximity and exchanges between the microorganisms and protected them. Poirier et al (2017) showed that different supports

mitigated the ammonia inhibition differently and the mitigation was associated to changes of the microbial community. The influence of the zeolite to facilitate electron transfer pathways should be further investigated, especially as *Peptococcaceae*, preserved by the zeolite, was recognised to be able to use DIET (Direct Electron Transfer) (Jing et al., 2017). The investigation of the functional pathways with metatranscriptomics analysis would provide further information on the microbial metabolism involved in presence of zeolite and ammonia.

4. Conclusion

This study evidenced the influence of the zeolite on the structuration of the anaerobic microbial population during a low stress caused by the presence of ammonia. Zeolite acted on the microbial distribution and allowed the growth of microorganisms like *Izimaplasmatales, Peptococcaceae* or *Methanobacterium*. The rearrangement of the community resulted in the modification of the equilibrium between the VFAs producers and degraders. Particularly, the syntrophic propionate and butyrate degradation were enhanced. The reasons for this rearrangement cannot be explained by the pre-treatments tested in our study as no strong modification between raw and modified zeolites could be observed. The effect seemed to be mostly due to the presence of a solid support. We hypothesize that it enabled the immobilisation of the biomass, inducing close interactions and protection, favourable in particular for the methanogens, and resulting in a limited deterioration of the bioprocess performances. Targeted analyses and the investigation of the microbial functions would allow to further understand the influence of zeolite on the syntrophic microbial metabolism.

Acknowledgements

This work was supported by the National Research Agency (grant number ANR-16-CE05-0014) as part of the Digestomic project. We want to thank Pierre-Antoine Bar,

Chrystelle Bureau, Angeline Guenne and Nadine Derlet from the Irstea PROSE analytical division for their technical support.

Funding

This work was conducted as part of the DIGESTOMIC project supported by the National Research Agency (ANR-16-CE05-0014). The funders had no role in study design, data collection and analysis, decision to publish, or preparation of the manuscript.

Bibliography

Abadzic, S.D., Ryan, J.N., 2001. Particle release and permeability reduction in a natural zeolite (clinoptilolite) and sand porous medium. Environ. Sci. Technol. 35, 4502–4508. https://doi.org/10.1021/es001868s

Anthonisen, A., Loehr, R., Prakasam, T., Srinath, E., 1976. Inhibition of Nitrification by Ammonia and Nitrous Acid. J. Water Pollut. Control Fed. 48, 835–852. https://doi.org/10.1017/CBO9781107415324.004

Astals, S., Peces, M., Batstone, D.J., Jensen, P.D., Tait, S., 2018. Characterising and modelling free ammonia and ammonium inhibition in anaerobic systems. Water Res. 143, 127–135. https://doi.org/10.1016/j.watres.2018.06.021

Ates, A., Hardacre, C., 2012. The effect of various treatment conditions on natural zeolites: Ion exchange, acidic, thermal and steam treatments. J. Colloid Interface Sci. 372, 130–140. https://doi.org/10.1016/j.jcis.2012.01.017

Bonk, F., Popp, D., Weinrich, S., Sträuber, H., Kleinsteuber, S., Harms, H., Centler, F., 2018. Ammonia inhibition of anaerobic volatile fatty acid degrading microbial communities. Front. Microbiol. 9, 1–13. https://doi.org/10.3389/fmicb.2018.02921

Bousek, J., Scroccaro, D., Sima, J., Weissenbacher, N., Fuchs, W., 2016. Influence of the gas composition on the efficiency of ammonia stripping of biogas digestate. Bioresour. Technol. 203, 259–266. https://doi.org/10.1016/j.biortech.2015.12.046

Calli, B., Mertoglu, B., Inanc, B., Yenigun, O., 2005. Effects of high free ammonia concentrations on the performances of anaerobic bioreactors. Process Biochem. 40, 1285–1292. https://doi.org/10.1016/j.procbio.2004.05.008

Capson-Tojo, G., Moscoviz, R., Astals, S., Robles, Steyer, J.P., 2020. Unraveling the literature chaos around free ammonia inhibition in anaerobic digestion. Renew. Sustain. Energy Rev. 117, 109487. https://doi.org/10.1016/j.rser.2019.109487

Cardona, L., Levrard, C., Guenne, A., Chapleur, O., Mazéas, L., 2019. Co-digestion of wastewater sludge: Choosing the optimal blend. Waste Manag. 87, 772–781. https://doi.org/10.1016/j.wasman.2019.03.016

579 Chapleur, O., Bize, A., Serain, T., Mazéas, L., Bouchez, T., 2014. Co-inoculating ruminal
580 content neither provides active hydrolytic microbes nor improves methanization of 13C-
581 cellulose in batch digesters. FEMS Microbiol. Ecol. 87, 616–629.
582 https://doi.org/10.1111/1574-6941.12249

583 Chen, Y., Cheng, J.J., Creamer, K.S., 2008. Inhibition of anaerobic digestion process: A
584 review. Bioresour. Technol. 99, 4044–4064.
585 https://doi.org/10.1016/j.biortech.2007.01.057

586 Escudié, F., Auer, L., Bernard, M., Mariadassou, M., Cauquil, L., Vidal, K., Maman, S.,
587 Hernandez-Raquet, G., Combes, S., Pascal, G., 2018. FROGS: Find, Rapidly, OTUs
588 with Galaxy Solution. Bioinformatics 34, 1287–1294.

589 Fernández, N., Montalvo, S., Fernández-Polanco, F., Guerrero, L., Cortés, I., Borja, R.,
590 Sánchez, E., Travieso, L., 2007. Real evidence about zeolite as microorganisms
591 immobilizer in anaerobic fluidized bed reactors. Process Biochem. 42, 721–728.
592 https://doi.org/10.1016/j.procbio.2006.12.004

593 Florentino, A.P., Sharaf, A., Zhang, L., Liu, Y., 2019. Overcoming ammonia inhibition in
594 anaerobic blackwater treatment with granular activated carbon: The role of electroactive
595 microorganisms. Environ. Sci. Water Res. Technol. 5, 383–396.
596 https://doi.org/10.1039/c8ew00599k

597 Hahnke, S., Langer, T., Koeck, D.E., Klocke, M., 2016. Description of Proteiniphilum
598 saccharofermentans sp. nov., Petrimonas mucosa sp. nov. and Fermentimonas caenicola
599 gen. nov., sp. nov., isolated from mesophilic laboratory-scale biogas reactors, and
600 emended description of the genus Proteiniphilum. Int. J. Syst. Evol. Microbiol. 66,
601 1466–1475. https://doi.org/10.1099/ijsem.0.000902

602 Hassa, J., Maus, I., Off, S., Pühler, A., Scherer, P., Klocke, M., Schlüter, A., 2018.
603 Metagenome, metatranscriptome, and metaproteome approaches unraveled compositions
604 and functional relationships of microbial communities residing in biogas plants. Appl.
605 Microbiol. Biotechnol. 102, 5045–5063. https://doi.org/10.1007/s00253-018-8976-7

606 Jarrell, K.F., Saulnier, M., Ley, A., 1987. Inhibition of methanogenesis in pure cultures by
607 ammonia, fatty acids, and heavy metals, and protection against heavy metal toxicity by
608 sewage sludge. Can. J. Microbiol. 33, 551–554.
609 https://doi.org/https://doi.org/10.1139/m87-093

610 Jing, Y., Wan, J., Angelidaki, I., Zhang, S., Luo, G., 2017. iTRAQ quantitative proteomic
611 analysis reveals the pathways for methanation of propionate facilitated by magnetite.
612 Water Res. 108, 212–221. https://doi.org/10.1016/j.watres.2016.10.077

613 Kesraoui-Ouki, S., Cheeseman, C.R., Perry, R., 1994. Natural Zeolite Utilization in Pollution
614 Control: A Review of Applications to Metals′ Effluents. J. Chem. Technol. Biotechnol.
615 59, 121–126. https://doi.org/10.1002/chin.199432295

616 Krakat, N., Anjum, R., Dietz, D., Demirel, B., 2017. Methods of ammonia removal in
617 anaerobic digestion: A review. Water Sci. Technol. 76, 1925–1938.
618 https://doi.org/10.2166/wst.2017.406

619 Lê Cao, K.-A., Costello, M.E., Lakis, V.A., Bartolo, F., Chua, X.Y., Brazeilles, R., Rondeau,
620 P., 2016. MixMC: A multivariate statistical framework to gain insight into microbial

621 communities. PLoS One 11. https://doi.org/10.1371/journal.pone.0160169

622 Lee, J., Kim, E., Han, G., Tongco, J.V., Shin, S.G., Hwang, S., 2018. Microbial communities
623 underpinning mesophilic anaerobic digesters treating food wastewater or sewage sludge:
624 A full-scale study. Bioresour. Technol. 259, 388–397.
625 https://doi.org/10.1016/j.biortech.2018.03.052

626 Lee, S.-H., Park, J.-H., Kang, H.-J., Lee, Y.H., Lee, T.J., Park, H.-D., 2013. Distribution and
627 abundance of Spirochaetes in full-scale anaerobic digesters. Bioresour. Technol. 145,
628 25–32. https://doi.org/10.1016/J.BIORTECH.2013.02.070

629 Lv, Z., Jiang, J., Liebetrau, J., Richnow, H.H., Fischer, A., Ács, N., Nikolausz, M., 2018.
630 Ammonium Chloride vs Urea-Induced Ammonia Inhibition of the Biogas Process
631 Assessed by Stable Isotope Analysis. Chem. Eng. Technol. 41, 671–679.
632 https://doi.org/10.1002/ceat.201700482

633 Madigou, C., Lê Cao, K.-A., Bureau, C., Mazéas, L., Déjean, S., Chapleur, O., 2019.
634 Ecological consequences of abrupt temperature changes in anaerobic digesters. Chem.
635 Eng. J. 361, 266–277. https://doi.org/10.1016/J.CEJ.2018.12.003

636 Mata-Alvarez, J., Dosta, J., Romero-Güiza, M.S., Fonoll, X., Peces, M., Astals, S., 2014. A
637 critical review on anaerobic co-digestion achievements between 2010 and 2013. Renew.
638 Sustain. Energy Rev. 36, 412–427. https://doi.org/10.1016/j.rser.2014.04.039

639 Milán, Z., Sánchez, E., Weiland, P., Borja, R., Martín, A., Ilangovan, K., 2001. Influence of
640 different natural zeolite concentrations on the anaerobic digestion of piggery waste.
641 Bioresour. Technol. 80, 37–43. https://doi.org/10.1016/S0960-8524(01)00064-5

642 Montalvo, S., Díaz, F., Guerrero, L., Sánchez, E., Borja, R., 2005. Effect of particle size and
643 doses of zeolite addition on anaerobic digestion processes of synthetic and piggery
644 wastes. Process Biochem. 40, 1475–1481. https://doi.org/10.1016/j.procbio.2004.06.032

645 Montalvo, S., Guerrero, L., Borja, R., Sánchez, E., Milán, Z., Cortés, I., Angeles de la la
646 Rubia, M., 2012. Application of natural zeolites in anaerobic digestion processes: A
647 review. Appl. Clay Sci. 58, 125–133. https://doi.org/10.1016/j.clay.2012.01.013

648 Müller, N., Worm, P., Schink, B., Stams, A.J.M., Plugge, C.M., 2010. Syntrophic butyrate
649 and propionate oxidation processes: From genomes to reaction mechanisms. Environ.
650 Microbiol. Rep. 2, 489–499. https://doi.org/10.1111/j.1758-2229.2010.00147.x

651 Munk, B., Guebitz, G.M., Lebuhn, M., 2017. Influence of nitrogen-rich substrates on biogas
652 production and on the methanogenic community under mesophilic and thermophilic
653 conditions. Anaerobe 46, 146–154. https://doi.org/10.1016/j.anaerobe.2017.02.015

654 Narihiro, T., Nobu, M.K., Tamaki, H., Kamagata, Y., Liu, W.-T., 2016. Draft Genome
655 Sequence of Syntrophomonas wolfei subsp . methylbutyratica Strain 4J5 T (JCM 14075
656), a Mesophilic Butyrate- and. Am. Soc. Microbiol. 4, 14075.
657 https://doi.org/10.1128/genomeA.00047-16.Copyright

658 Poirier, S., Déjean, S., Midoux, C., Lê Cao, K.-A., Chapleur, O., 2020. Integrating
659 independent microbial studies to build predictive models of anaerobic digestion
660 inhibition. bioRxiv. https://doi.org/https://doi.org/10.1101/2020.03.16.993220

661 Poirier, S., Desmond-Le Quéméner, E., Madigou, C., Bouchez, T., Chapleur, O., 2016.

662 Anaerobic digestion of biowaste under extreme ammonia concentration: Identification of
663 key microbial phylotypes. Bioresour. Technol. 207, 92–101.
664 https://doi.org/10.1016/j.biortech.2016.01.124

665 Poirier, S., Madigou, C., Bouchez, T., Chapleur, O., 2017. Improving anaerobic digestion
666 with support media: Mitigation of ammonia inhibition and effect on microbial
667 communities. Bioresour. Technol. 235, 229–239.
668 https://doi.org/10.1016/j.biortech.2017.03.099

669 Prabhu, M.S., Mutnuri, S., 2016. Anaerobic co-digestion of sewage sludge and food waste.
670 Waste Manag. Res. 34, 307–315.

671 Rajagopal, R., Massé, D.I., Singh, G., 2013. A critical review on inhibition of anaerobic
672 digestion process by excess ammonia. Bioresour. Technol. 143, 632–641.
673 https://doi.org/10.1016/j.biortech.2013.06.030

674 Rivière, D., Desvignes, V., Pelletier, E., Chaussonnerie, S., Guermazi, S., Weissenbach, J., Li,
675 T., Camacho, P., Sghir, A., 2009. Towards the definition of a core of microorganisms
676 involved in anaerobic digestion of sludge. ISME J. 3, 700–714.
677 https://doi.org/10.1038/ismej.2009.2

678 Rohart, F., Gautier, B., Singh, A., Cao, K.-A. Le, 2017. mixOmics: an R package for 'omics
679 feature selection and multiple data integration. bioRxiv 108597.
680 https://doi.org/10.1101/108597

681 Ruiz-Sánchez, J., Campanaro, S., Guivernau, M., Fernández, B., Prenafeta-Boldú, F.X., 2018.
682 Effect of ammonia on the active microbiome and metagenome from stable full-scale
683 digesters. Bioresour. Technol. 250, 513–522.
684 https://doi.org/10.1016/j.biortech.2017.11.068

685 Ruiz-Sánchez, J., Guivernau, M., Fernández, B., Vila, J., Viñas, M., Riau, V., Prenafeta-
686 Boldú, F.X., 2019. Functional biodiversity and plasticity of methanogenic biomass from
687 a full-scale mesophilic anaerobic digester treating nitrogen-rich agricultural wastes. Sci.
688 Total Environ. 649, 760–769. https://doi.org/10.1016/j.scitotenv.2018.08.165

689 Schnurer, A., Nordberg, A., 2008. Ammonia, a selective agent for methane production by
690 syntrophic acetate oxidation at mesophilic temperature. Water Sci. Technol. 57, 735–
691 740.

692 Skennerton, C.T., Haroon, M.F., Briegel, A., Shi, J., Jensen, G.J., Tyson, G.W., Orphan, V.J.,
693 2016. Phylogenomic analysis of Candidatus "Izimaplasma" species: Free-living
694 representatives from a Tenericutes clade found in methane seeps. ISME J. 10, 2679–
695 2692. https://doi.org/10.1038/ismej.2016.55

696 Sousa, D.Z., Smidt, H., Alves, M.M., Stams, A.J.M., 2009. Ecophysiology of syntrophic
697 communities that degrade saturated and unsaturated long-chain fatty acids. FEMS
698 Microbiol. Ecol. 68, 257–272. https://doi.org/10.1111/j.1574-6941.2009.00680.x

699 Tada, C., Yang, Y., Hanaoka, T., Sonoda, A., Ooi, K., Sawayama, S., 2005. Effect of natural
700 zeolite on methane production for anaerobic digestion of ammonium rich organic sludge.
701 Bioresour. Technol. 96, 459–464. https://doi.org/10.1016/j.biortech.2004.05.025

702 Tian, H., Mancini, E., Treu, L., Angelidaki, I., Fotidis, I.A., 2019. Bioaugmentation strategy
703 for overcoming ammonia inhibition during biomethanation of a protein-rich substrate.

704 Chemosphere 231, 415–422. https://doi.org/10.1016/j.chemosphere.2019.05.140

705 Ueki, A., Akasaka, H., Suzuki, D., Ueki, K., 2006. Paludibacter propionicigenes gen. nov., sp.
706 nov., a novel strictly anaerobic, Gram-negative, propionate-producing bacterium isolated
707 from plant residue in irrigated rice-field soil in Japan. Int. J. Syst. Evol. Microbiol. 56,
708 39–44. https://doi.org/10.1099/ijs.0.63896-0

709 Wang, H., Fotidis, I.A., Angelidaki, I., 2015. Ammonia effect on hydrogenotrophic
710 methanogens and syntrophic acetate-oxidizing bacteria. FEMS Microbiol. Ecol. 91, 1–8.
711 https://doi.org/10.1093/femsec/fiv130

712 Wang, Q., Yang, Y., Yu, C., Huang, H., Kim, M., Feng, C., Zhang, Z., 2011. Study on a fixed
713 zeolite bioreactor for anaerobic digestion of ammonium-rich swine wastes. Bioresour.
714 Technol. 102, 7064–7068. https://doi.org/10.1016/j.biortech.2011.04.085

715 Weiß, S., Lebuhn, M., Andrade, D., Zankel, A., Cardinale, M., Birner-Gruenberger, R.,
716 Somitsch, W., Ueberbacher, B.J., Guebitz, G.M., 2013. Activated zeolite - Suitable
717 carriers for microorganisms in anaerobic digestion processes? Appl. Microbiol.
718 Biotechnol. 97, 3225–3238. https://doi.org/10.1007/s00253-013-4691-6

719 Weiß, S., Zankel, A., Lebuhn, M., Petrak, S., Somitsch, W., Guebitz, G.M., 2011.
720 Investigation of mircroorganisms colonising activated zeolites during anaerobic biogas
721 production from grass silage. Bioresour. Technol. 102, 4353–4359.
722 https://doi.org/10.1016/j.biortech.2010.12.076

723 Westerholm, M., Moestedt, J., Schnürer, A., 2016. Biogas production through syntrophic
724 acetate oxidation and deliberate operating strategies for improved digester performance.
725 Appl. Energy 179, 124–135. https://doi.org/10.1016/j.apenergy.2016.06.061

726 Westerholm, M., Müller, B., Arthurson, V., Schnürer, A., 2011. Changes in the Acetogenic
727 Population in a Mesophilic Anaerobic Digester in Response to Increasing Ammonia
728 Concentration. Microbes Environ. 26, 347–353. https://doi.org/10.1264/jsme2.ME11123

729 Whiticar, M.J., Faber, E., Schoell, M., 1986. Biogenic methane formation in marine and
730 freshwater environments: CO2reduction vs. acetate fermentation-Isotope evidence.
731 Geochim. Cosmochim. Acta 50, 693–709. https://doi.org/10.1016/0016-7037(86)90346-
732 7

733 Wijesinghe, D.T.N., Dassanayake, K.B., Sommer, S.G., Scales, P., Chen, D., 2019. Biogas
734 Improvement by Adding Australian Zeolite During the Anaerobic Digestion of C:N
735 Ratio Adjusted Swine Manure. Waste and Biomass Valorization 10, 1883–1887.
736 https://doi.org/10.1007/s12649-018-0210-4

737 Wu, Y., Wang, C., Liu, X., Ma, H., Wu, J., Zuo, J., Wang, K., 2016. A new method of two-
738 phase anaerobic digestion for fruit and vegetable waste treatment. Bioresour. Technol.
739 211, 16–23. https://doi.org/10.1016/j.biortech.2016.03.050

740 Yang, Z., Wang, W., Liu, C., Zhang, R., Liu, G., 2019. Mitigation of ammonia inhibition
741 through bioaugmentation with different microorganisms during anaerobic digestion:
742 Selection of strains and reactor performance evaluation. Water Res. 155, 214–224.
743 https://doi.org/10.1016/j.watres.2019.02.048

744 Yenigün, O., Demirel, B., 2013. Ammonia inhibition in anaerobic digestion: A review.
745 Process Biochem. 48, 901–911. https://doi.org/10.1016/j.procbio.2013.04.012

Yi, J., Dong, B., Jin, J., Dai, X., 2014. Effect of increasing total solids contents on anaerobic digestion of food waste under mesophilic conditions: Performance and microbial characteristics analysis. PLoS One 9. https://doi.org/10.1371/journal.pone.0102548

Zhang, C., Yuan, Q., Lu, Y., 2018. Inhibitory effects of ammonia on syntrophic propionate oxidation in anaerobic digester sludge. Water Res. 146, 275–287. https://doi.org/10.1016/j.watres.2018.09.046

Zhang, N., Zheng, H., Hu, X., Zhu, Q., Stanislaus, M.S., Li, S., Zhao, C., Wang, Q., Yang, Y., 2019. Enhanced bio-methane production from ammonium-rich waste using eggshell-and lignite-modified zeolite (ELMZ) as a bio-adsorbent during anaerobic digestion. Process Biochem. 81, 148–155. https://doi.org/10.1016/j.procbio.2019.03.001

Ziganshin, A.M., Schmidt, T., Scholwin, F., Il'Inskaya, O.N., Harms, H., Kleinsteuber, S., 2011. Bacteria and archaea involved in anaerobic digestion of distillers grains with solubles. Appl. Microbiol. Biotechnol. 89, 2039–2052. https://doi.org/10.1007/s00253-010-2981-9

Zou, B.-Z., Takeda, K., Tonouchi, A., Akada, S., Fujita, T., 2003. Characteristics of an Anaerobic, Syntrophic, Butyrate-degrading Bacterium in Paddy Field Soil. Biosci. Biotechnol. Biochem. 67, 2059–2067. https://doi.org/10.1271/bbb.67.2059

Figures legends:

Table 1. Experimental set-up.

Figure 1. Comparison of the Gompertz parameters (maximal production, production rate and lag phase) for both CO_2 and CH_4 for the different conditions. Each black point represents one digester. Red triangles represent the mean for each condition. Green point represents the mean of all samples (Grand Mean). The different conditions are labelled on the top. Digesters with ammonia are named N and digesters without ammonia are named C**.** The number corresponds to the different conditions of zeolite 0: no zeolite, 1: raw zeolite, 2: liquid residue, 3: solid residue, 4: heated zeolite. Conditions are ordered according to the contrast coefficient represented on the x-axis. The range of the values of the parameter is represented on the left in addition to the value of the Grand Mean and its standard deviation. The values of the group means are represented on the right. The blue square represents the area of the mean square root error within the conditions. The red square represents the area of the mean square root error between the conditions. The F-statistic and p-value are indicated. F-statistic value is the ratio of the area MS-within and of the MS-between. The residuals are represented as a blue line reported on the right of the y-axis. A- ANOVA of the CO_2 maximal production. B- ANOVA of the CO_2 production rate. C- ANOVA of the CO_2 lag phase. D- ANOVA of the CH_4 maximal production. E- ANOVA of the CH_4 production rate. F- ANOVA of the CH_4 lag phase.

Figure 2. Evolution of the chemical parameters. The data are the mean values for the triplicate bioreactors, standard deviations are indicated

Figure 3. Methanogenic pathway measured through the isotopic fractionation of the CH4 (δ13C-CH4). The data are the mean values for the triplicate bioreactors, standard deviations are indicated.

Figure 4. Abundances of the most discriminant microorganisms in the digesters under ammonia inhibition. This heatmap represents the OTUs (column) selected after 3 pair-wise sparse Partial Least Square Discriminant Analysis (sPLS-DA) on the samples (row) to discriminate the different types of digesters. The colour of the heatmap represents the abundances of the OTUs after centered log ratio transformation. Taxonomic affiliation is presented at the family level for the bacteria and genus level for the archaea. Arrows indicate remarkable OTUs.

Figure 5. Summary of the hypothetical pathways of degradation for the different conditions. Molecules which accumulated and methanogenesis pathways involved during the degradation are highlighted in blue. Specific microorganisms identified with the sparse PLS-DA are represented inside a rectangle and situated in the pathway where we supposed they were active. The role of the microorganisms between question marks is unknown. Genus Mbac: *Methanobacterium; Msar: Methanosarcina; Mc: Methanoculleus;* Orders Lac: *Lachnospiraceae*; Spi: *Spirochaetaceae*; Cloa: *Cloacimonadaceae*; Rik: *Rikenellaceae*; Pal: *Paludibacteraceae*; Pep: *Peptococcaceae; Syn: Syntrophomonadaceae*; Mari: *Marinilabiliaceae*; Family Izi: *Izimaplasmatales*

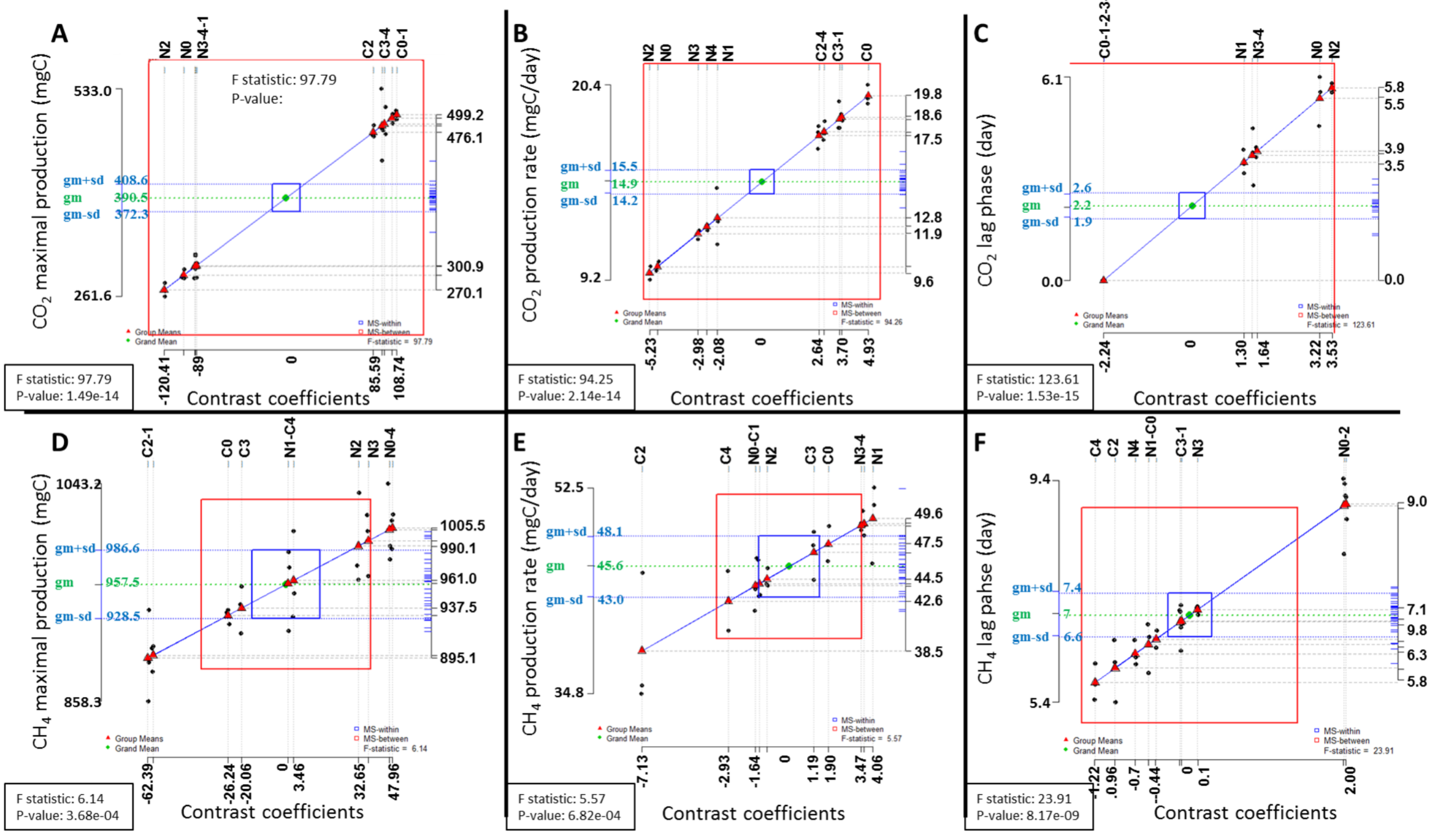
A
N2 N0 N3-4-1 C2 C3-4 C0-1
F statistic: 97.79
P-value:
533.0
261.6
gm+sd 408.6
gm 390.5
gm-sd 372.3
499.2
476.1
300.9
270.1
CO2 maximal production (mgC)
Group Means
Grand Mean
MS-within
MS-between
F-statistic = 97.79
-120.41 -89 0 85.59 108.74
Contrast coefficients
F statistic: 97.79
P-value: 1.49e-14
B
N2 N0 N3 N4 N1 C2-4 C3-1 C0
20.4
9.2
gm+sd 15.5
gm 14.9
gm-sd 14.2
19.8
18.6
17.5
12.8
11.9
9.6
CO2 production rate (mgC/day)
Group Means
Grand Mean
MS-within
MS-between
F-statistic = 94.26
-5.23 -2.98 -2.08 0 2.64 3.70 4.93
Contrast coefficients
F statistic: 94.25
P-value: 2.14e-14
C
C0-1-2-3-4 N1 N3-4 N0 N2
6.1
0.0
gm+sd 2.6
gm 2.2
gm-sd 1.9
5.8
5.5
3.9
3.5
0.0
CO2 lag phase (day)
Group Means
Grand Mean
MS-within
MS-between
F-statistic = 123.61
-2.24 0 1.30 1.64 3.22 3.53
Contrast coefficients
F statistic: 123.61
P-value: 1.53e-15
D
C2-1 C0 C3 N1-C4 N2 N3 N0-4
1043.2
858.3
gm+sd 986.6
gm 957.5
gm-sd 928.5
1005.5
990.1
961.0
937.5
895.1
CH4 maximal production (mgC)
Group Means
Grand Mean
MS-within
MS-between
F-statistic = 6.14
-62.39 -26.24 -20.06 0 3.46 32.65 47.96
Contrast coefficients
F statistic: 6.14
P-value: 3.68e-04
E
C2 C4 N0-C1 N2 C3 C0 N3-4 N1
52.5
34.8
gm+sd 48.1
gm 45.6
gm-sd 43.0
49.6
47.5
44.5
42.6
38.5
CH4 production rate (mgC/day)
Group Means
Grand Mean
MS-within
MS-between
F-statistic = 5.57
-7.13 -2.93 -1.64 0 1.19 1.90 3.47 4.06
Contrast coefficients
F statistic: 5.57
P-value: 6.82e-04
F
C4 C2 N4 N1-C0 C3-1 N3 N0-2
9.4
5.4
gm+sd 7.4
gm 7
gm-sd 6.6
9.0
7.1
9.8
6.3
5.8
CH4 lag pahse (day)
Group Means
Grand Mean
MS-within
MS-between
F-statistic = 23.91
-1.22 -0.96 -0.7 -0.44 0 0.1 2.00
Contrast coefficients
F statistic: 23.91
P-value: 8.17e-09

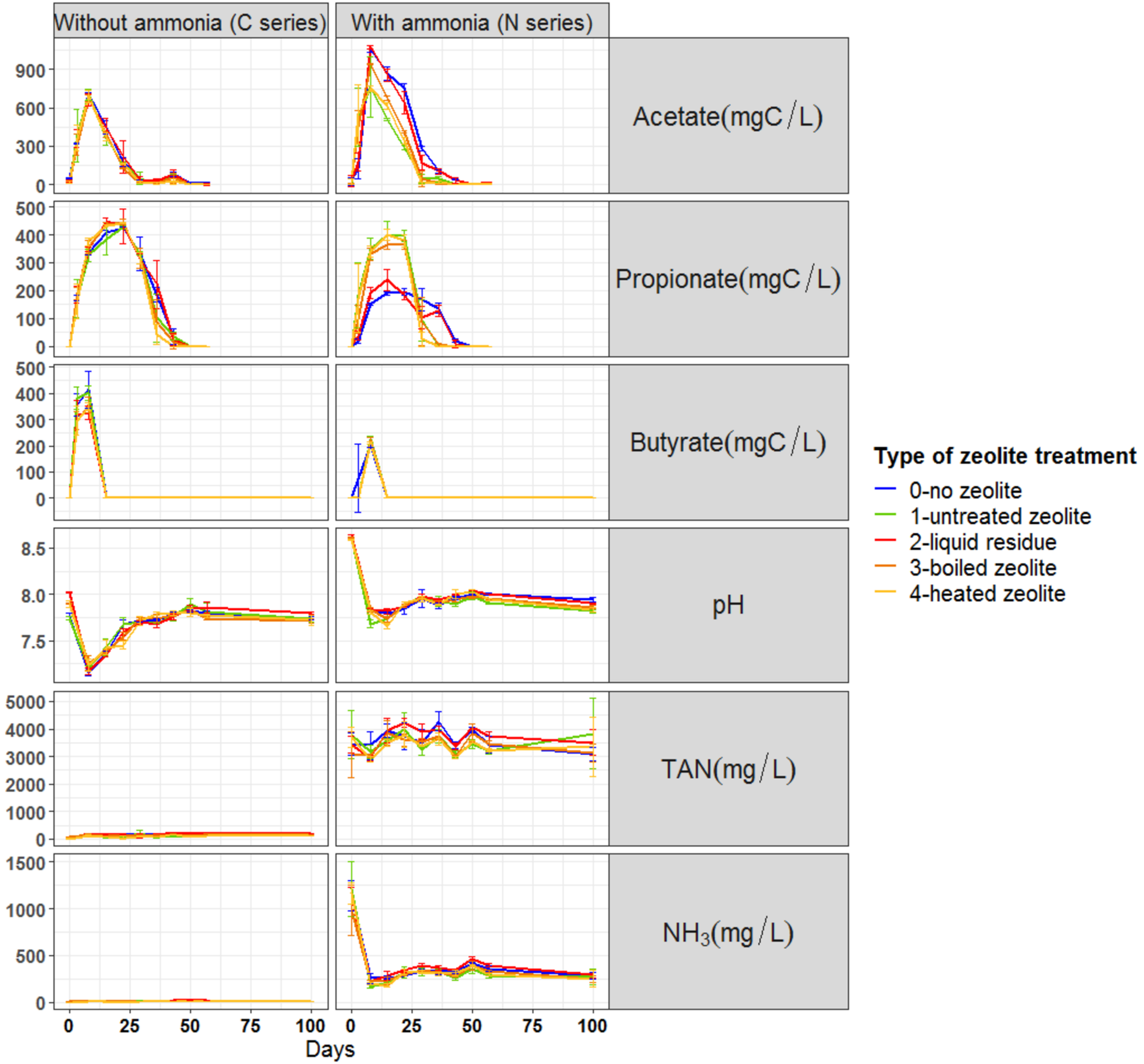
Without ammonia (C series)
With ammonia (N series)
Acetate(mgC/L)
Propionate(mgC/L)
Butyrate(mgC/L)
pH
TAN(mg/L)
NH3(mg/L)
Days
Type of zeolite treatment
0-no zeolite
1-untreated zeolite
2-liquid residue
3-boiled zeolite
4-heated zeolite

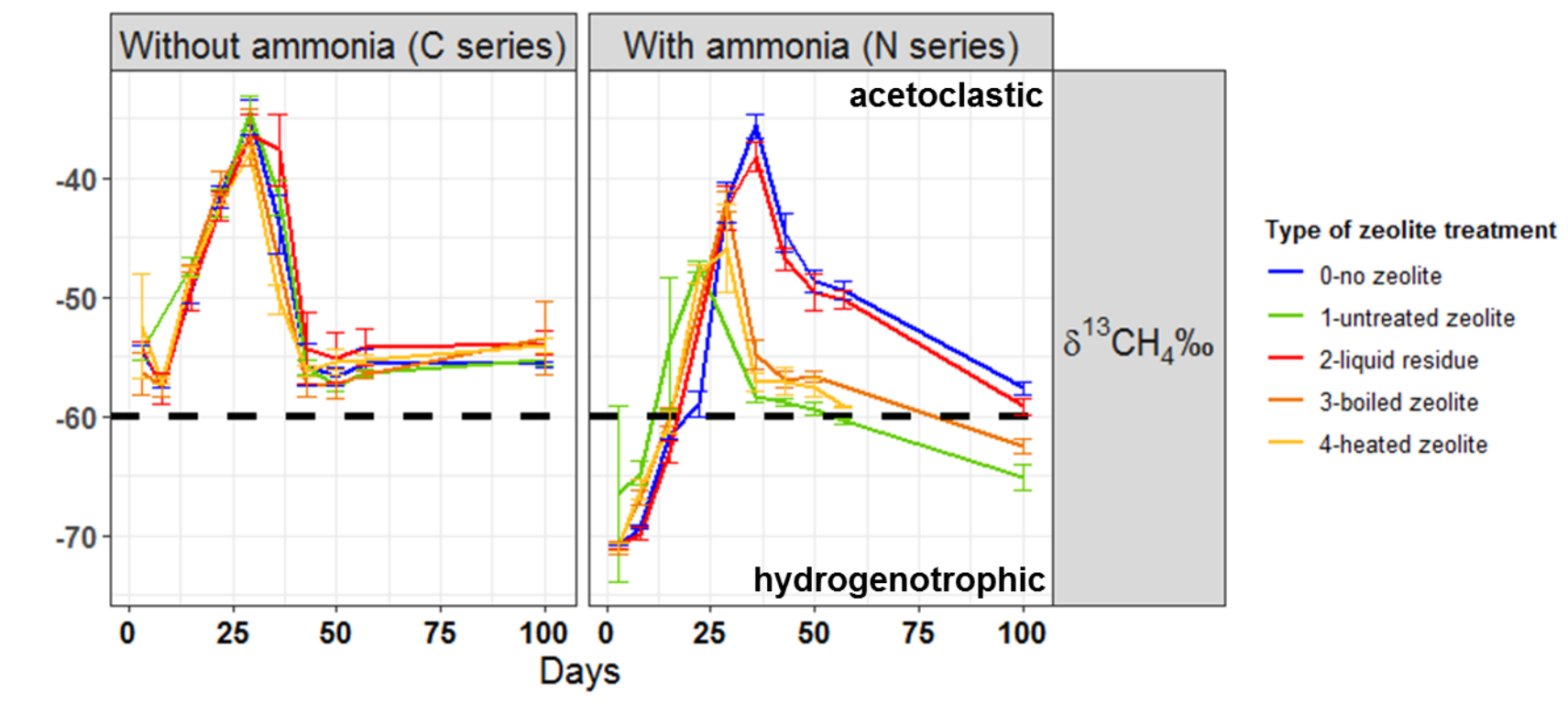
Without ammonia (C series)
With ammonia (N series)
acetoclastic
hydrogenotrophic
δ13CH4‰
-40
-50
-60
-70
0
25
50
75
100
Days
Type of zeolite treatment
0-no zeolite
1-untreated zeolite
2-liquid residue
3-boiled zeolite
4-heated zeolite

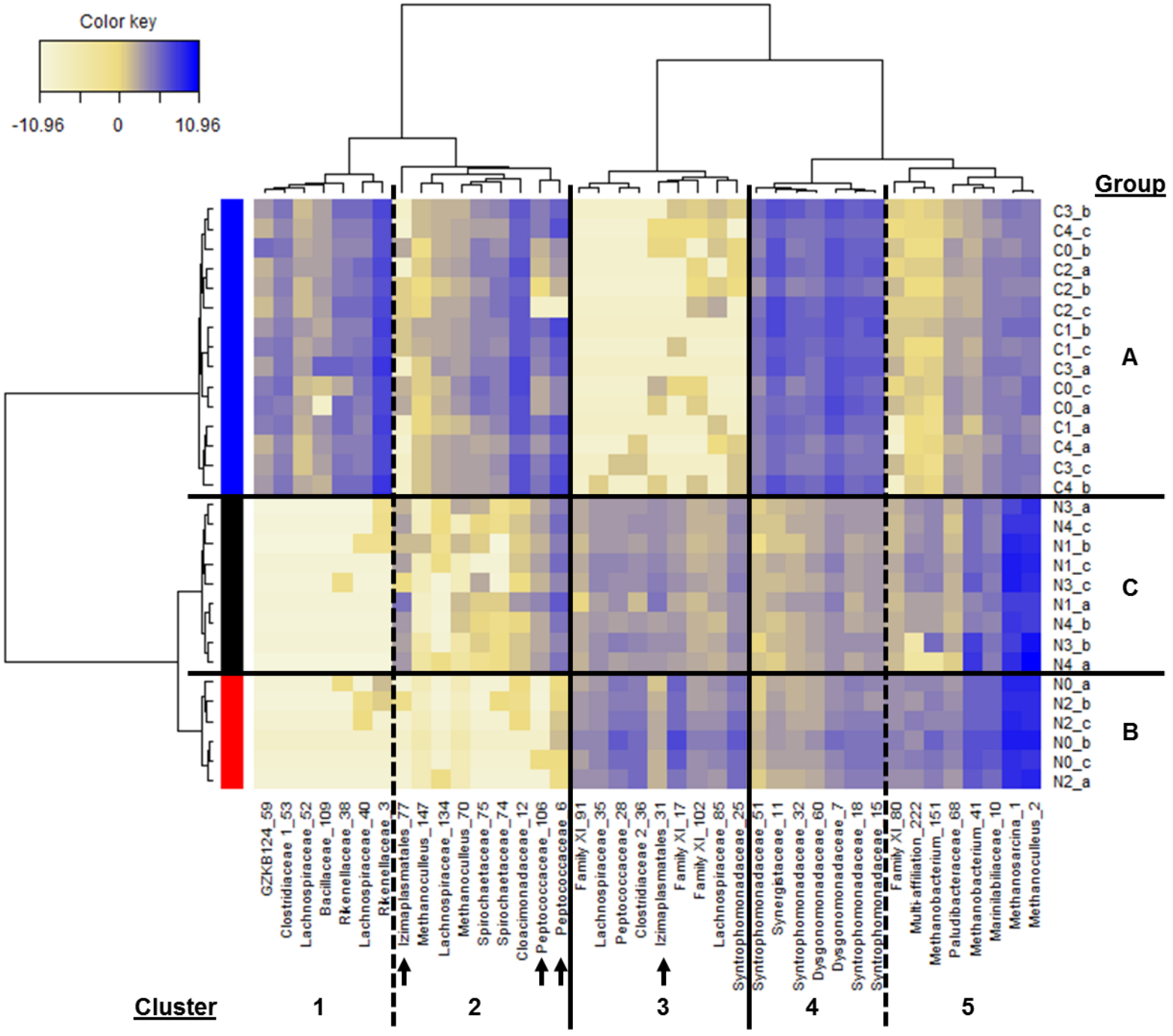
Color key
-10.96
0
10.96
Group
C3_b
C4_c
C0_b
C2_a
C2_b
C2_c
C1_b
C1_c
C3_a
C0_c
C0_a
C1_a
C4_a
C3_c
C4_b
A
N3_a
N4_c
N1_b
N1_c
N3_c
N1_a
N4_b
N3_b
N4_a
C
N0_a
N2_b
N2_c
N0_b
N0_c
N2_a
B
GZKB124_59
Clostridiaceae 1_53
Lachnospiraceae_52
Bacillaceae_109
Rikenellaceae_38
Lachnospiraceae_40
Rikenellaceae_3
Izimaplasmatales_77
Methanoculleus_147
Lachnospiraceae_134
Methanoculleus_70
Spirochaetaceae_75
Spirochaetaceae_74
Cloacimonadaceae_12
Peptococcaceae_106
Peptococcaceae_6
Family XI_91
Lachnospiraceae_35
Peptococcaceae_28
Clostridiaceae 2_36
Izimaplasmatales_31
Family XI_17
Family XI_102
Lachnospiraceae_85
Syntrophomonadaceae_25
Syntrophomonadaceae_51
Synergistaceae_11
Syntrophomonadaceae_32
Dysgonomonadaceae_60
Dysgonomonadaceae_7
Syntrophomonadaceae_18
Syntrophomonadaceae_15
Family XI_80
Multi-affiliation_222
Methanobacterium_151
Paludibacteraceae_68
Methanobacterium_41
Marinilabiliaceae_10
Methanosarcina_1
Methanoculleus_2
Cluster
1
2
3
4
5

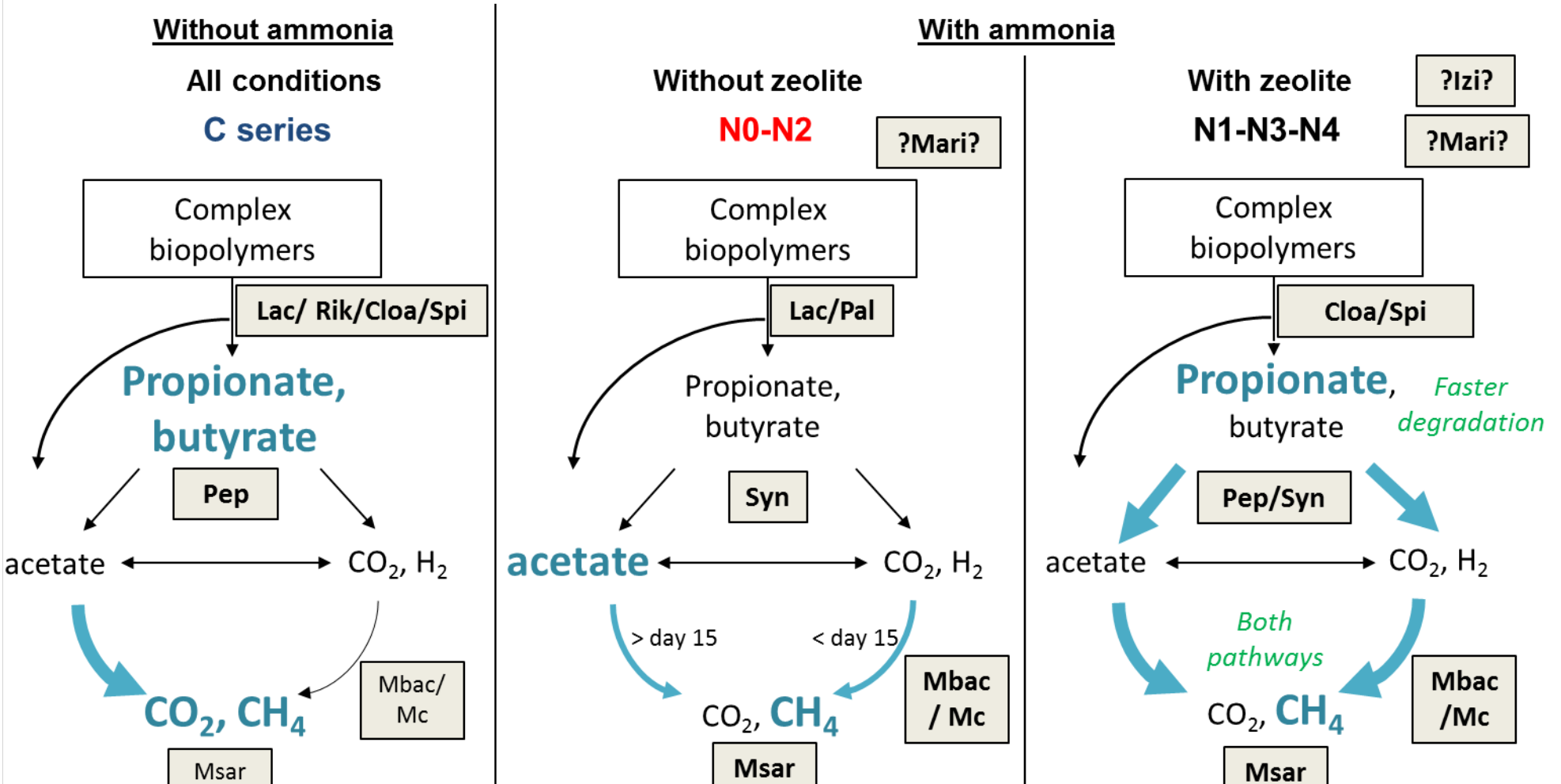
Without ammonia
All conditions
C series
Complex biopolymers
Lac/ Rik/Cloa/Spi
Propionate, butyrate
Pep
acetate
CO2, H2
CO2, CH4
Mbac/ Mc
Msar
With ammonia
Without zeolite
N0-N2
?Mari?
Complex biopolymers
Lac/Pal
Propionate, butyrate
Syn
acetate
CO2, H2
> day 15
< day 15
CO2, CH4
Mbac / Mc
Msar
With zeolite
?Izi?
?Mari?
N1-N3-N4
Complex biopolymers
Cloa/Spi
Propionate, butyrate
Faster degradation
Pep/Syn
acetate
CO2, H2
Both pathways
CO2, CH4
Mbac /Mc
Msar

Ammonia	Reactor	Zeolite type	Sludge (g)	Biowaste (g)	$(NH_4)_2CO_3$ (g)	Zeolite (g)
4 g/L NH_4^+	N0	No zeolite	4	29	11	0
	N1	Untreated zeolite	4	29	11	11
	N2	Liquid residue after boiling zeolite at 100°C, filtered 0.22µm	4	29	11	11
	N3	Solid residue after boiling zeolite at 100°C	4	29	11	11
	N4	Heated 400°C	4	29	11	11
0 g/L NH_4^+	C0	No zeolite	4	29	0	0
	C1	Untreated zeolite	4	29	0	11
	C2	Liquid residue after boiling zeolite at 100°C, filtered 0.22µm	4	29	0	11
	C3	Solid residue after boiling zeolite at 100°C	4	29	0	11
	C4	Heated 400°C	4	29	0	11

Batch experiments

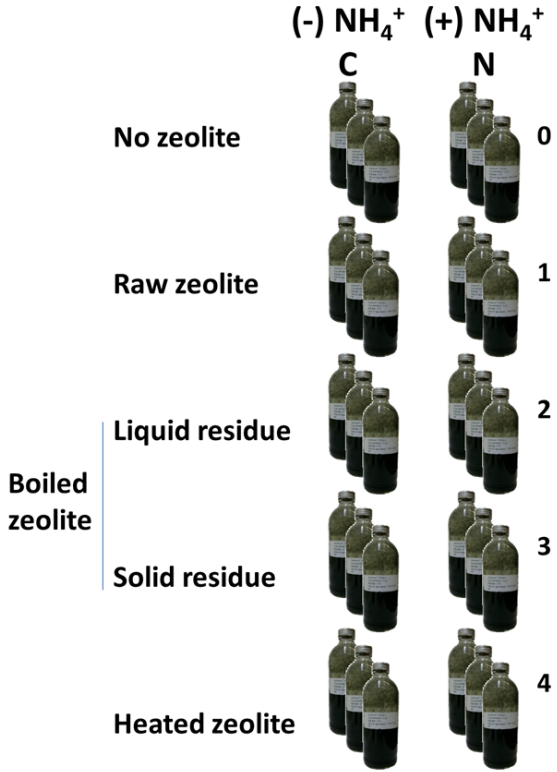

Methanogenic pathways and microbial diversity

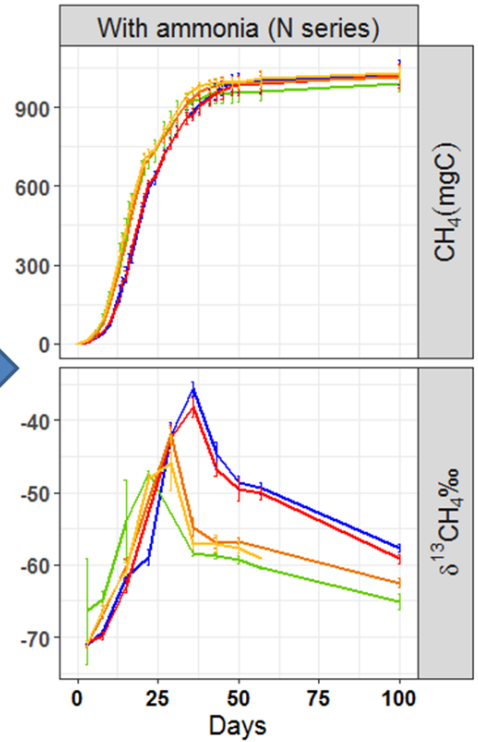

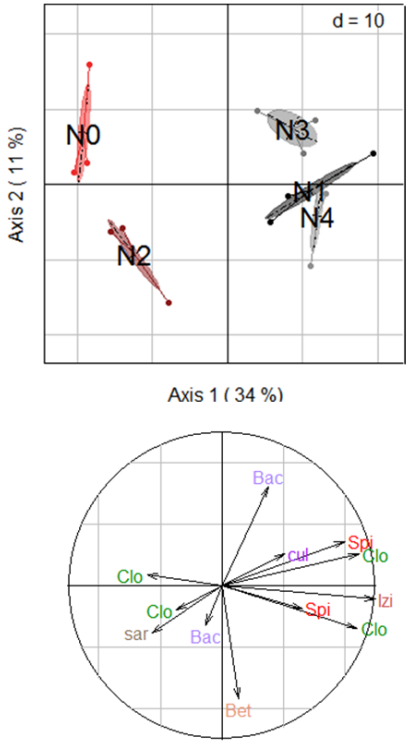

Pathway reconstruction